

PROCEEDINGS OF SPIE

[SPIDigitalLibrary.org/conference-proceedings-of-spie](https://spiedigitallibrary.org/conference-proceedings-of-spie)

Recent advance in phase transition of vanadium oxide based solar reflectors and the fabrication progress

Golsa Mirbagheri, David Crouse, Chee-Keong Tan

Golsa Mirbagheri, David T. Crouse, Chee-Keong Tan, "Recent advance in phase transition of vanadium oxide based solar reflectors and the fabrication progress," Proc. SPIE 11995, Physics and Simulation of Optoelectronic Devices XXX, 119950O (4 March 2022); doi: 10.1117/12.2626406

SPIE.

Event: SPIE OPTO, 2022, San Francisco, California, United States

Recent advance in phase transition of vanadium oxide based solar reflectors and the fabrication progress

Golsa Mirbagheri¹, David T. Crouse², Chee-Keong Tan²

*Duke University Pratt School of Engineering¹
Computer and Electrical Department of Clarkson University²*

ABSTARCT

Vanadium dioxide (VO₂) as a phase-change material controls the transferred heat during phase transition process between metal and insulator states. At temperature above 68 °C, the rutile structure VO₂ keeps the heat out and increases the IR radiation reflectivity, while at the lower temperature the monoclinic structure VO₂ acts as the transparent material and increase the transmission radiation. In this paper, we first present the metal-insulator phase transition (MIT) of the VO₂ in high and low temperatures. Then we simulate the meta-surface VO₂ of metamaterial reflector by Ansys HFSS to show the emittance tunability ($\Delta\epsilon$) of the rutile and monoclinic phase of the VO₂. In next section, we will review the recent progress in the deposition of thermochromic VO₂ on glass and silicon substrate with modifying the pressure of sputtering gases and temperature of the substrate. Finally, we present the results of the in-situ sputtered VO_x thin film on thick SiO₂ substrate in different combination of oxygen and argon environment by V₂O₅ target at temperature higher than 300°C and then, analyze it with x-ray diffraction (XRD) method. The thermochromic VO₂ based metamaterial structures open a new route to the passive energy-efficient optical solar reflector in the past few years.

Keywords: Nanofabrication, Phase Transition Metamaterial, V₂O₅ target, Optical Solar Reflector, Vanadium Oxide

1. INTRODUCTION

The reversible metal-insulator phase transition (MIT) of VO₂ has gained enormous attention in thermal control system of spacecrafts recently. However, among other metamaterials great effort is still investigated to understand the MIT process. In this section we review the recent advance in MIT mechanism of VO₂ and discuss the physical properties of the rutile and monoclinic structures. V-O system is one of the most interesting materials with different compounds including VO, VO₂, V₂O₃, V₃O₅, etc. Some of these components show metal-insulator transition (MIT) with a big change in thermal, optical, or electrical properties. These special properties encouraged scientists to use the V-O system in many optical applications and therefore, learn the phase transition process. Among all various types of V-O system, VO₂ is considered for the temperature phase change mechanism [1, 2, 3]. Today, great effort has been made to understand the MIT phase change mechanism on various VO₂ morphologies acquired from different types of fabrication methods. [4, 5, 6]. Despite the great progress has been made in recent years, the phase transition is still an arguable mechanism. The rapid transition between rutile metallic phase and monoclinic insulator phase is followed by changes in the crystallographic and electrical properties of VO₂, accomplished by switching and sensing applications [7].

The isolator behavior of VO₂ with 3d₁ orbital occupancy in room temperature and, forming other isolator phases in specific temperatures, all make it hard to interpret the phase change properties. One explanation for this change can be described by Peierls mechanism and electron correlation technique, which address the lattice distortion and the band gap shift. On the other hand, in the 3d t_{2g}-derived states of the vanadium, when d₁ bands break into occupied

¹ Send correspondence to Golsa Mirbagheri
E-mail: gm226@duke.edu

bonding and empty antibonding, the π^* states get depopulated and their energy increase that leads to create the bandgap. Therefore, a bandgap is created between the $d_{||}$ and the π^* bands, illustrated in Figure 1. However, bandgap disappear in rutile phase to allow reflection of radiations. Therefore, we explain the lattice structures and electron interaction to learn more about the transition process.

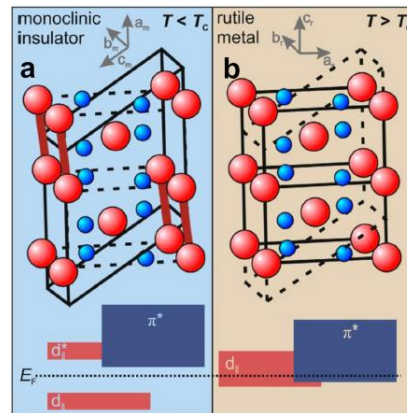


Figure 1. Bandgap in monoclinic (left) and rutile (right) phase of V [1]

The VO_2 can grow in the form of different crystal structures, including monoclinic (M) and rutile (R) phases which show reversible phase change close to room temperature. During the phase change, the d-electrons of V atoms in the symmetrical structure join to the varying V-V bonds in low symmetry monoclinic structure. There is an assumption that this V-V localized structure derived from the high temperature delocalized phase and shows insulative properties. On the other hand, the conductivity property in the high temperature rutile phase is due to the fermi level between the π^* band and the $d_{||}$ band. While in M phase, the $d_{||}$ band split to two parts, make a gap between $d_{||}$ band and the π^* band where Fermi level falls into that and lead to VO_2 to be insulative. However, this theory is no clarified yet, since some research show that lattice distortion is not the only reason for MIT phase transition. One hypothesis is that there are other phases rather than M, at the low temperature. With the help of doping, electron injection or stress effect, different phases of VO_2 like M2 monoclinic, triclinic VO_2 (T) or other metastable monoclinic metal phases are discovered, which indicated that V-V bond interactions is not the necessary step to open an insulating gap [1, 8, 9, 10]. Studying the transition phase of thermochromic VO_2 makes a new path to understand the correlation effects of other thermal sensors [11, 12, 13].

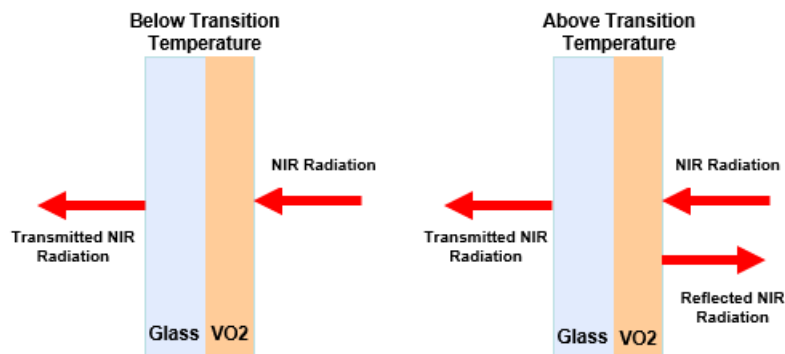


Figure 2. Vanadium dioxide semiconductor (left) to metal (right) phase transition at 68 °C shows change in infrared reflectivity

As a thermochromic material, VO_2 goes through semiconductor to metal phase transition at the specific temperature of 68 °C which makes the change in infrared reflectivity, as shown in Figure 2. The transmission radiation changes with temperature and thickness of the VO_2 material, which is demonstrated in Figure 3. The broadest extensive hysteresis transition belongs to the thickest VO_2 with 50nm. By increasing the temperature above 68 °C at wavelength

of 2 μm , the material keeps the heat out and IR radiation reflection increased since little radiation is transmitted into. To manipulate the transition temperature of the VO_2 film different method were introduces including the adding various dopants, using multiple layers, or size effectiveness of VO_2 lattice [14, 15, 16, 17].

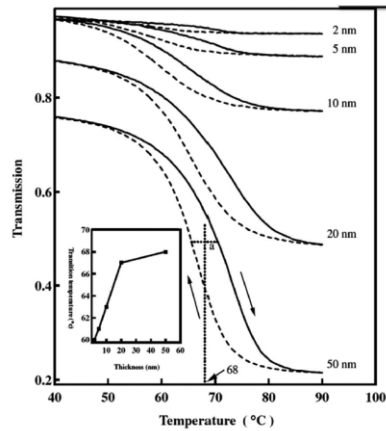


Figure 3. Transmission hysteresis loops for different thickness of VO_2 thin film at wavelength $2\mu\text{m}$ [14]

2. NUMERICAL SIMULATION OF FILTER

In [18], the optical solar reflector (OSR) composed of plasmonic VO_2 meta-surface is introduced to control the temperature of the satellite devices. The grating thermochromic VO_2 in the OSR filter improve the absorption (α) and emittance tunability $\Delta\epsilon$ with the help of plasmonic and thermochromic properties of VO_2 . This leads to higher absorption of the structure in higher temperature and lower absorption in temperature below the critical level. The smart meta-surface reflector shows higher tunability $\Delta\epsilon$ at lower absorptance in comparison with the planar thin film design [19]. The OSR reflects the radiation of the sun and dissipates the thermal spectrum of onboard instruments to reduce the solar absorption and keep down the thermal fluctuation of the satellite. In contrast with active systems, the smart passive systems keep the heat at low temperature (low emittance) and dissipates extra heat at high temperature (high emittance) to keep the temperature at optimal ranges. This makes the passive systems cost and energy effective with lower weight. In passive thermal control structures, thermochromic VO_2 works as a reflector and shows semiconductor to metal phase change at specific temperature 68°C with high tunability of emittance. The critical temperature can be manipulated by doping or defect engineering methods to be near room temperature. The performance of the passive smart system can be explained by the dynamic emittance tunability of $\Delta\epsilon = \epsilon_{\text{hot}} - \epsilon_{\text{cold}}$. VO_2 based metamaterials exhibits phase transmission on plasmonic effects that shows higher absorption in metallic state and lower emittance in monoclinic phase, applicable over a wide range from visible and NIR to MWIR. The insulator SiO_2 in [18] is sandwiched between the meta-surface VO_2 and aluminum reflector, shown in Figure 4, makes the destructive interference effect to improve the blackbody spectrum absorption and high tunability $\Delta\epsilon$. The Al_2O_3 layer is considered as adhesion material.

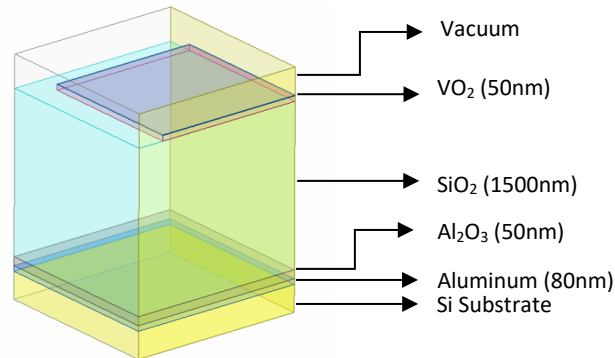


Figure 4. VO_2 based OSR Schematic Simulated in HFSS

The proposed structure is composed of the array of metasurface VO₂ in the shape of the square grating and simulated by Ansys HFSS, demonstrated in Figure 4. The absorption infrared spectra of the monoclinic grating VO₂ with grating squares size 2.8μm and different gaps between grating square changes from 3.3-4.35μm at temperature 30°C is low at 5-7μm and 12-18μm which is illustrated in Figure 5.

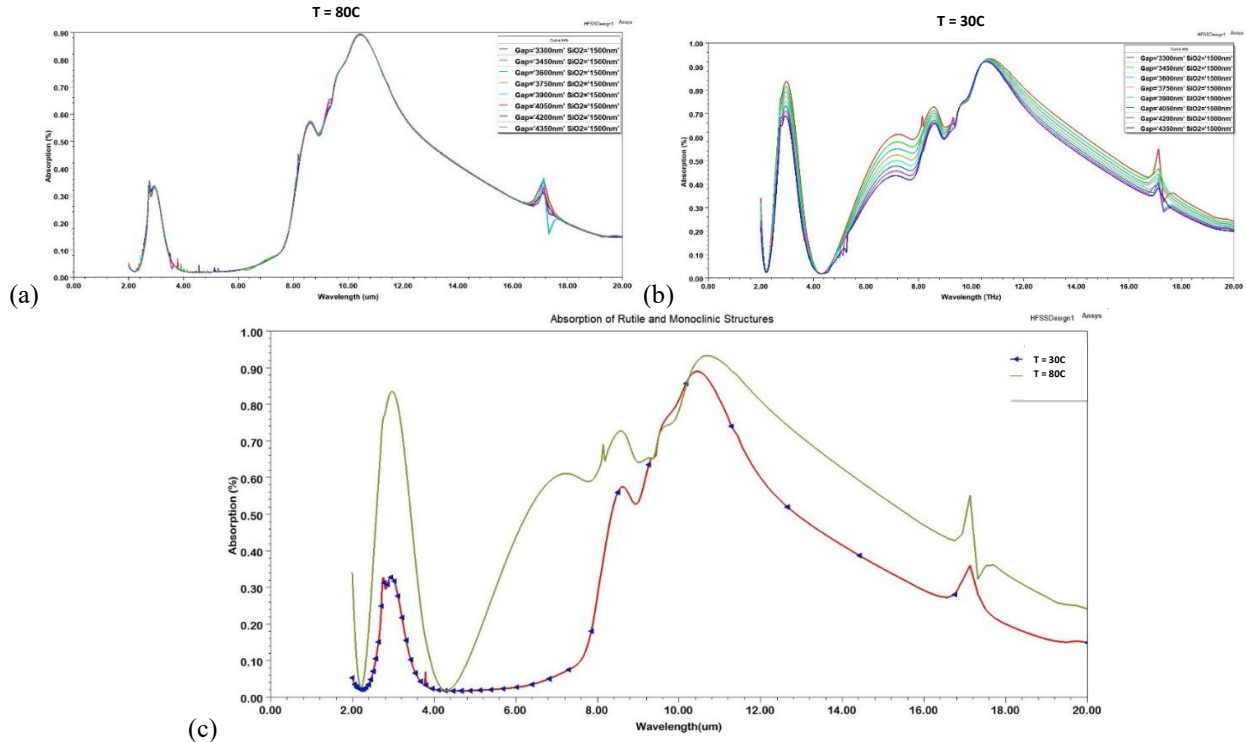


Figure 5. Absorption of meta surface VO₂ at 30°C (a) and at 80°C (b). Comparison of absorption of meta surface VO₂ between two rutile and monoclinic structures of grating VO₂ based metamaterial structure (c)

The emittance of a reflector is described in Eq. 1 as the average emittance weighted by blackbody spectrum at temperature (T).

$$\varepsilon = \frac{\int (1-R(\lambda))B(\lambda, T)d\lambda}{B(\lambda, T)d\lambda} \quad (1) [18]$$

Using Eq 1, the emittance of the meta-surface VO₂ with low-emissivity dielectric spacer in high and low temperature is calculated by the measuring the reflection spectra from FTIR method, as shown in Figure 6 (a). Therefore, it's not hard to find the emittance tunability $\Delta\varepsilon$ of the meta-surface VO₂ at the peak of the blackbody spectrum, which is plotted in Figure 6 (b). The latter shows that by increasing the gap size between features (or decreasing the feature size of the grating VO₂), maximum emittance tunability $\Delta\varepsilon$ improved about %30 in comparison with the planar film of VO₂.

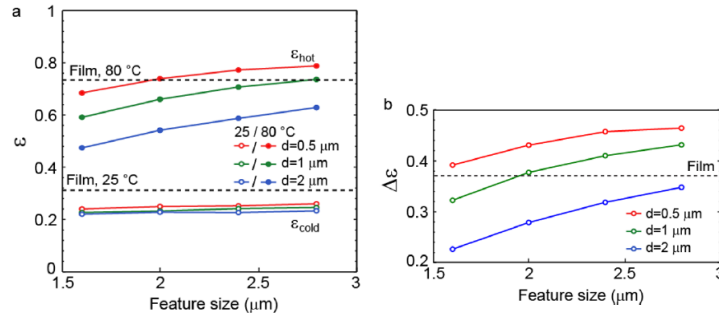


Figure 6. Measured emittance (left) and emittance tunability (right) of planar film (dash line) and meta-surface VO₂ for high and low temperatures [18]

3. REVIEW OF RECENT VO₂ DEPOSITION WORKS

In the recent years, different methods were advised to sputter vanadium films [20, 21, 22]. In order to make thermochromic VO₂ of metamaterial structures, we review some deposition approaches with the help of modifying the pressure of gases and temperature of the substrate [23, 24, 25]. One method is to sputter thin film with vanadium target and then oxidized it in high temperature annealing environment at temperature 300 °C or above. The other popular way is reactive sputtering deposition which is performed with the partial oxygen pressure %0 to %20 of the total pressure (argon/oxygen atmosphere) at 300-600 °C to create different mixtures of VO_x (V₂O₃, V₂O₅ or VO₂) on the substrate. The films can be analyzed with XRD, atomic force microscopy and X-ray photon spectroscopy (XPS) methods, in addition to checking the color of different composition of VO_x visually [26]. Furthermore, post annealing in 300 °C or higher is recommended to form various types of VO_x in other works. In [23], different forms of VO_x were deposited on substrate with RF magnetron deposition by V₂O₅ target at temperature 300 to 527 °C without annealing process. At the oxygen partial pressure less than 10⁻³³ in room temperature in RF magnet deposition process, the VO₂ is the most stable phase of the other composition of VO_x from the V₂O₅ target. The VO₂ thin film deposited on the glass substrate at 125W plasma power with the oxygen partial pressure changing from 0-20% of argon/oxygen for 100 minutes. Meanwhile, at the oxygen partial pressure higher than 10⁻²⁹, V₂O₅ grows on the substrate as shown in Figure 7 [23, 27, 28].

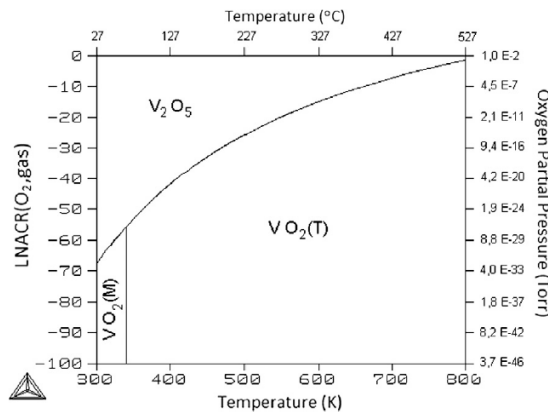


Figure 7. Monoclinic (M) and tetragonal (T) VO₂ and V₂O₅ thin films growth from V₂O₅ target at partial oxygen pressures [23]

Reactive hydrogen is used for Rf sputtering of vanadium film with V₂O₅ target to reduce oxygen, whereas reactive oxygen is suggested for metallic vanadium or V₂O₃ target. The V₂O₃ target provides broader flow ratio during sputtering vanadium oxide, but it is more expensive than other two targets. Furthermore, metallic target gets oxidized during sputtering process, therefore, V₂O₅ is the most stable and best sputtering target to deposit rutile VO₂. However, due to safety requirement, reactive oxygen is recommended with V₂O₅ target at higher temperature. In [24], rutile VO₂ is deposited on fused silica glasses, Si or thick SiO₂ on Si substrate from a V₂O₅ target by tuning substrate temperature and the oxygen flow rate. The temperature of substrate changed from 300 to 500 °C during the deposition with the total

oxygen/argon pressure 12.5 mTorr at the power of 60 or 120W and the oxygen flow ratio (R_{f_0}) is adjusted between 0.042 to 0.1 based on Eq 2, where f is the flow rate of the gas.

$$R_{f_0} = \frac{f_{O_2}}{(f_{Ar} + f_{O_2})} \quad (2) [24]$$

The temperature of the substrate plays an important role for adjusting the oxygen component of the thin film. Figure 8 shows at lower temperature 300 °C, the V_4O_9 phase starts to grow on Si substrate. As temperature increases, V_6O_{13} and meta-stable phase VO_2 (A) phases show at $R_{f_0} = 0.1$ due to less oxygen content of the films. Other phases with lower oxygen grow on the Si substrate when R_{f_0} is decreased. At higher temperature 500°C, only rutile VO_2 grows on the Si substrate with R_{f_0} between 0.06 and 0.042 in power 60W.

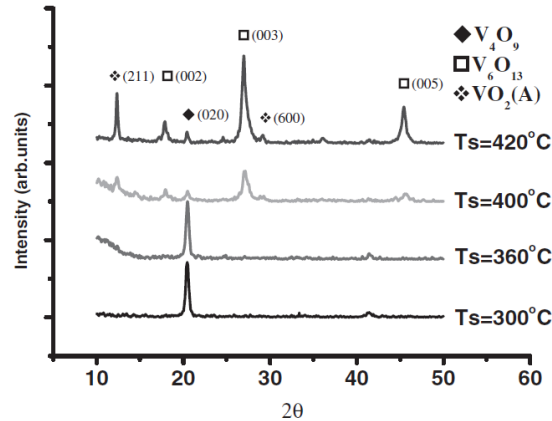


Figure 8. XRD result of thin films on Si substrate at different temperature from 300°C to 420°C for $R_{f_0} = 0.3$ [24]

Figure 9 shows that the increasing the temperature of substrate not only form the phases with lower oxygen, but also increase the average grain size of the deposited thin film.

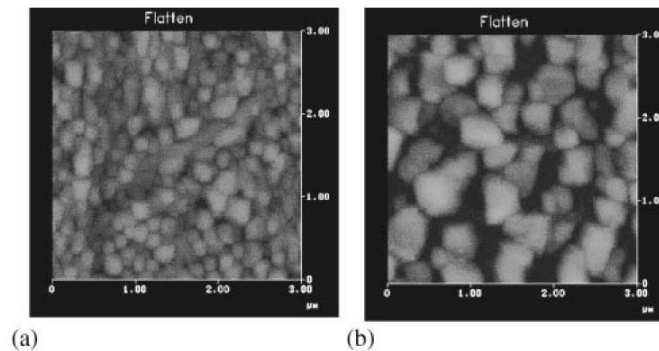


Figure 9. AFM results for grain sizes of mixed rutile VO_2 and VO_2 (A) phases at $T = 450^\circ\text{C}$ (left) vs single phase rutile VO_2 film at $T = 500^\circ\text{C}$ (right) [24]

In [25], VO_2 is sputtered from V_2O_5 target with reactive hydrogen (2.5-10% of H_2+Ar) at pressure 0.2 Pa and power 100W. After 30 min pre-sputtering, the temperature of the fused silica glass substrate kept at 400 °C to grow the VO_2 smoothly. In [29], the deposited precursor vanadium on the SiO_2/Si substrate with metal vanadium target is oxidized to VO_2 in chamber at temperature 370-415°C and oxygen pressure 0.2Torr. Furthermore, post annealing at 270 °C (better result at 450 °C) is an alternative method to oxidize the deposited vanadium to shape the VO_2 . However, the best results were related to the in-situ deposition immediately after deposition of precursor vanadium. In [30], the single (001) orientation orthorhombic metal vanadium is in situ deposited on sapphire, silicon, and glass substrates by RF sputtering with vanadium target in partial oxygen pressure 0-25% at temperature less than 100°C. In [31], the deposited vanadium post-annealed at 530°C with an oxygen pressure between 14 -18 Pa to not oxidize changing to

V₂O₅. In [32], the phase transition of VO₂ is improved by further post-annealing at 300°C in high-pressure oxygen 10–25 mTorr. The XRD result in Figure 10, shows thin film VO₂ sputtered by pulsed laser deposition (PLD) method on thick oxide (SiO₂/Si) substrate [33].

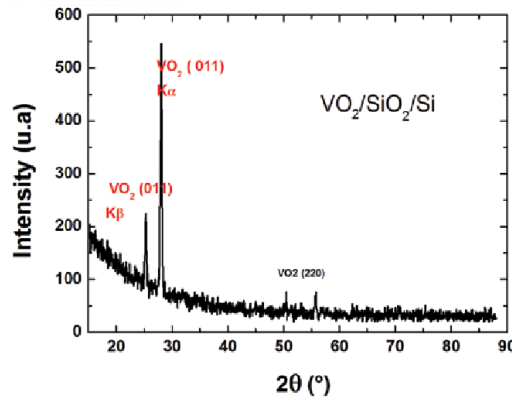


Figure 10. XRD results for VO₂ film deposited on SiO₂/Si substrate [33]

4. EXPERIMENTAL RESULT

In our work, we sputtered 50nm VO_x film on SiO₂/Si substrate by V₂O₅ target. The substrate is composed of 1.5µm thermal SiO₂ deposited on silicon wafer by plasma-enhanced chemical vapor deposition (PECVD) method. During RF sputtering process, total gas pressure was kept at 12.5 mTorr for 2hours deposition process. We did several sputtering tests for different temperature of substrate varied from 300°C to 500°C in-situ at a power of 120W for different oxygen and argon flow ratio. The wafer height in the chamber held 20cm from target. The surface of the thin film is characterized by XRD at temperatures 300°C, 400°C and 500°C in Figure 11, shows that for flow ratio O₂= 2sccm and Ar(P) = 32sccm (R_{f0} 0.058), the deposited film on thick SiO₂ is V₂O₃. We repeated the test for R_{f0} between 0.042 to 0.06, however the measured surface of the thin film by XRD technique showed V₂O₃ growth on the thick oxide substrate. The result did not change significantly after post-annealing process for partial oxygen pressure 100Torr at 300°C, 400°C and 500°C. For the total volume of oxygen and nitrogen equal to 10 lit/min, %13 oxygen (1.3 lit/min) and %43 nitrogen (8.6 lit/min) were considered to do post-anneal the sputter film about 10 minutes. In [34], the ALD deposited amorphous vanadium oxide crystallized in furnace annealing process in higher rate of nitrogen ratio (more than %98) at temperature of 425°C and higher, as shown in Table 1 [35, 36, 37, 38]. The gray rows in Table 1 show the successful annealing process of create polycrystalline stoichiometric VO₂ phase.

Anneal Temp	Air	Annealing time and gas ratio under atmospheric pressure				Annealing time and gas ratio under low vacuum (10 ⁻² Torr)		
		N ₂ (100%)	98.78% N ₂ + 1.22% O ₂	99% N ₂ + 1% O ₂	98.5% N ₂ + 1.5% O ₂	98.2% N ₂ + 1.8% O ₂	99.4% N ₂ + 0.6% O ₂	2.7×10 ⁻² Torr (1 sccm O ₂)
420°C	30 min							
420°C		30 min						
420°C				5 min				
420°C					5 min			
420°C						10 min		
420°C							10 min	
425°C			30 min					
430°C				5 min				
450°C	30 min							
450°C		30 min						
450°C				30 min				
450°C					5 min			
450°C						10 min		
450°C							10 min	
500°C								60 min

Table 1. The furnace annealing result to crystallize the ALD deposited amorphous vanadium oxide film [34]

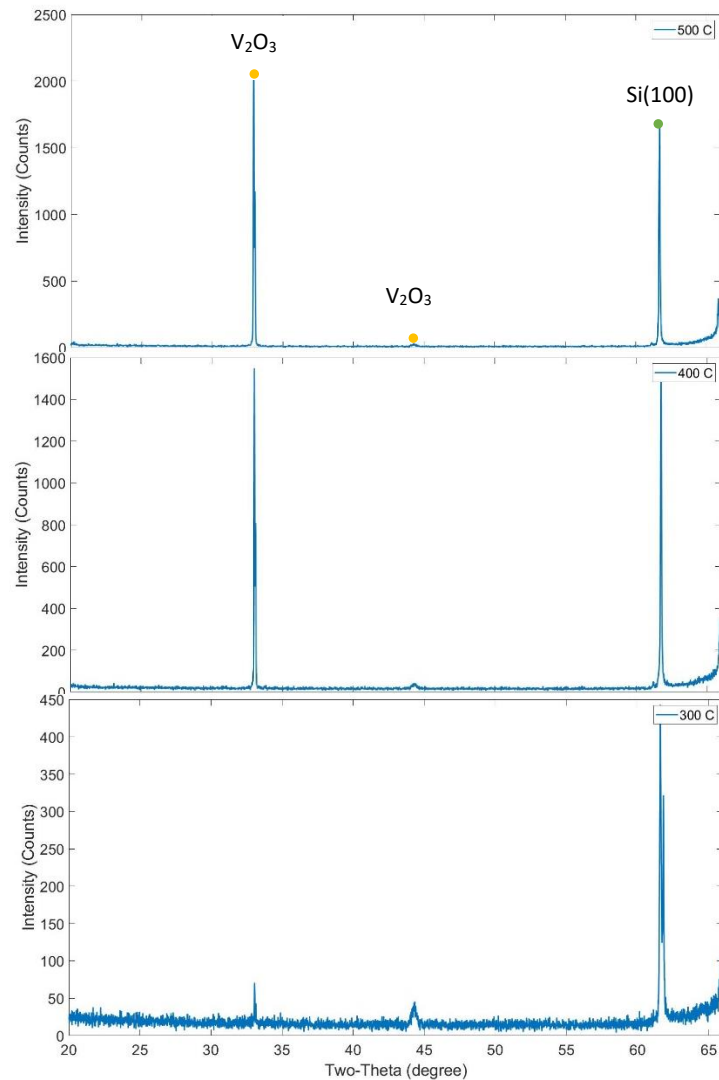


Figure 11. XRD result for sputtered film with Rfo 0.058 at temperature from 300°C (bottom), 400°C (middle) and 500°C (top)

5. CONCLUSION

In this article, the crystallographic and electrical properties of VO₂ were reviewed to show the metal-insulator phase transition of the film at temperature 68 °C. The proposed VO₂ based metamaterial structure was simulated with HFSS to demonstrate the emittance tunability ($\Delta\epsilon$) of rutile and monoclinic states of VO₂. We summarized the recent progress in the in the deposition of thermochromic VO₂ on glass and silicon substrate by focusing on changing the partial pressure of the oxygen and argon. Furthermore, we sputtered VO_x by V₂O₅ target with Rfo between 0.042 to 0.6 at temperature 300°C and higher and measured it with XRD method, which resulted in forming the V₂O₃ on the thick oxide on silicon wafer. For future work, it is recommended to sputter the thin film VO_x on sapphire or silicon substrate with V₂O₃, since VO₂ grows smoothly on sapphire in comparison with the thick thermal SiO₂. Thin films thermochromic vanadium dioxide is currently attracting much attention in areas such as microelectronics and spacecraft control systems for their electronic behaviors in MIT.

6. ACKNOWLEDGEMENT

This work was performed in part at the Cornell NanoScale Facility, a member of the National Nanotechnology Coordinated Infrastructure (NNCI), which is supported by the National Science Foundation (Grant NNCI-2025233). Also, we appreciate the Cornell Center for Materials Research Shared Facilities which are supported through the NSF MRSEC program (DMR-1719875). We would like to thank the NSF Industry/University Cooperative Research Center for Metamaterials to support this project.

7. REFERENCES

- [1] Shao Z., Cao X., Luo H. and Jin P., "Recent progress in the phase-transition mechanism and modulation of vanadium dioxide materials," *NPG Asia Materials*, vol. 10, pp. 581-605, (2018).
- [2] Zhao B. and Zhang Z. M., "Design of Optical and Radiative Properties of Surfaces," *Springer International Publishing AG*, (2017).
- [3] sitoga.eu, "VANADIUM DIOXIDE," PERFORMANCE, SILICON CMOS COMPATIBLE TRANSITION METAL OXIDE TECHNOLOGY FOR BOOSTING HIGHLY INTEGRATED PHOTONIC DEVICES WITH DISRUPTIVE, (2013).
- [4] Mirbagheri G., Dunn K. J., Kosciolk D. J., Bendoym I. and Crouse D. T., "Hyperbolic metamaterial filter for angle-independent TM transmission in the infrared regime (Conference Presentation)," in *SPIE Nanoscience + Engineering*, San Diego, California, United States, vol. 103431U, (2017).
- [5] Mirbagheri G., Crouse D. T., Dunn K. and Bendoym I., "Metamaterials based hyperspectral and multi-wavelength filters for imaging applications," *SPIE Defense + Commercial Sensing*, vol. 109800A, (2019).
- [6] Mirbagheri G., "Hyperbolic Metamaterial Filter for Angle-Independent TM-Transmission in Imaging Applications," Proquest, Potsdam, NY. US, (2020).
- [7] Mirbagheri G. and Crouse D. T., " Design, fabrication, and spectral characterization of temperature-dependent liquid crystal-based metamaterial to tune dielectric metasurface resonances," *SPIE Photonics West OPTO*, (2022).
- [8] Jin Y., "REACTIVE SPUTTER DEPOSITION OF VANADIUM, NICKEL, AND MOLYBDENUM OXIDE THIN FILMS FOR USE IN UNCOOLED INFRARED IMAGING," The Pennsylvania State University, The Graduate School, Department of Engineering Science and Mechanics, Philadelphia, PA, (2014).
- [9] Wu S.R., Lai K.L. and Wang C.M., "Passive temperature control based on a phase change metasurface," *Scientific REPOrTS*, vol. 8, no. 7684, (2018).
- [10] Shelton D., Coffey K. and Boreman G. D., "Experimental demonstration of tunable phase in a thermochromic infrared-reflectarray metamaterial," *OPTICS EXPRESS*, vol. 18, no. 2, pp. 1330-1335, (2010).
- [11] Ito K., Watari T., Nishikawa K., Yoshimoto H. and Iizuka H., "Inverting the thermal radiative contrast of vanadium dioxide by metasurfaces based on localized gap-plasmons," *APL PHOTONICS*, vol. 3, no. 086101 , (2018).
- [12] Shin J.H., Moon K., Lee E. S., Lee I.M. and Park K. H., "Metal-VO₂ hybrid grating structure for a terahertz active switchable linear polarizer," *Nanotechnology*, vol. 26 , no. 315203 , p. 7pp, (2015).
- [13] Mirbagheri G. and Crouse D. T., " Design, fabrication, and spectral characterization of TM-polarized metamaterials-based narrowband infrared filter," *SPIE Photonics West OPTO*, (2022).
- [14] Warwick M. E. A. and Binions R., "Advances in thermochromic vanadium dioxide films," *The Royal Society of Chemistry*, p. 3275–3292, (2014).
- [15] Eyert V., "VO₂: A novel view from band theory," *Physical Review Letters* , (2011).

- [16] Kim H., Cheung K., R. C. .. Auyeung Y., Wilson D. E., Charipar K. M., Piqué A. and Charipar N. A., "VO₂-based switchable radiator for spacecraft thermal control," *Scientific Reports*, vol. 9, no. 11329, (2019).
- [17] LEI L., LOU F., TAO K., HUANG H., CHENG X. and XU P., "Tunable and scalable broadband metamaterial absorber involving VO₂-based phase transition," *Photonics Research*, vol. 7, no. 7, pp. 734-741, (2019).
- [18] Sun K., Riedel C. A., Urbani A., Simeoni M., Mengali S., Zalkovskij M., Bilenberg B., Groot C. d. and Muskens O. L., "VO₂ Thermochromic Metamaterial-Based Smart Optical Solar Reflector," *ACS Photonics*, vol. 5, no. 6, p. 2280–2286, (2018).
- [19] Hamaoui G., Horny N., Gomez-Heredia C. L., Ramirez-Rincon J. A., Ordonez-Miranda J., Champeaux C., Dumas-Bouchiat F., Alvarado-Gil J. J., Ezzahri Y., Joulain K. and Chirtoc M., "Thermophysical characterisation of VO₂ thin films hysteresis and its application in thermal rectification," *Scientific Reports*, vol. 9, no. 8728, (2019).
- [20] Ho H.C., Lai Y.C., Chen K. and C.H. Thang Duy Dao H. N., "High quality thermochromic VO₂ films prepared by magnetron sputtering using V₂O₅ target with in situ annealing," *Applied Surface Science*, vol. 495, no. 143436, (2019).
- [21] Fangfang Song B. E. W. J., "Growth of ultra thin vanadium dioxide thin films using magnetron sputtering," Department of Physics, Applied Physics, Astronomy, Binghamton University - State University of New York, Binghamton, NY.
- [22] Giannetta H. M. R., Calaza C., Fraigi L. and Fonseca L., "Vanadium Oxide Thin Films Obtained by Thermal Annealing of Layers Deposited by RF Magnetron Sputtering at Room Temperature," *Licensee InTech*, pp. 152-168, (2017).
- [23] Castro M. S. d., Ferreira C. L. and Avillez R. R. d., "Vanadium oxide thin films produced by magnetron sputtering from a V₂O₅ target at room temperature," *Infrared Physics & Technology*, vol. 60, p. 103–107, (2013).
- [24] TSAI K.Y., CHIN T.S. and SHIEH H.P. D., "Properties of VO₂ Films Sputter-Deposited from V₂O₅ Target," *The Japan Society of Applied Physics*, vol. 42, p. 4480–4483, (2003).
- [25] SHIGESATO Y., ENOMOTO M. and ODAKA H., "Thermochromic VO₂ Films Deposited by RF Magnetron Sputtering Using V₂O₃ or V₂O₅ Targets," *The Japan Society of Applied Physics*, vol. 39, p. 6016–6024, (2000).
- [26] CURRIE M., MASTRO M. A. and WHEELER V. D., "Characterizing the tunable refractive index of vanadium dioxide," *OPTICAL MATERIALS EXPRESS*, vol. 7, no. 5, pp. 1697-1707, (2017).
- [27] Kusano E. and Theil J., "Deposition of vanadium oxide films by direct-current magnetron reactive," *Journal of Vacuum Science & Technology A Vacuum Surfaces and Films*, vol. 6, no. 3, (1988).
- [28] DAI K., LIAN J., MILLER M. J., WANG J., SHI Y., LIU Y., SONG H. and WANG X., "Optical properties of VO₂ thin films deposited on different glass substrates," *OPTICAL MATERIALS EXPRESS*, vol. 9, no. 2, pp. 663-672, (2019).
- [29] Gurvitch M., Luryi S., Polyakov A., Shabalov A., Dudley M., Wang G., Ge S. and Yakovlev V., "VO₂ films with strong semiconductor to metal phase transition prepared by the precursor oxidation process," *J. Appl. Phys.*, vol. 102, p. 033504, (2007).
- [30] Hansen S. D. and Aita C. R., "Low temperature reactive sputter deposition of vanadium oxide," *Journal of Vacuum Science & Technology*, vol. 3, pp. 660-663, (1985).
- [31] Liu X., Wang S.W., Chen F., Yu L. and Chen X., "Tuning phase transition temperature of VO₂ thin films by annealing atmosphere," *Journal of Physics D: Applied Physics*, vol. 48, no. 265104, (2015).
- [32] Song F. and B. E. W. Jr., "Growth control of the oxidation state in vanadium oxide thin films," *Materials Science*, (2016).

- [33] Hassein-Beya A. L. S., Lafanea S., Tahib H., Hassein-Bey A., Djafara A. A., Abdelli-Messacia S. and Benamard M. E. A., "Substrate Effect on Structural, Microstructural and Elemental Microcomposition of Vanadium Dioxide Thin Film," *Modern Arabic Review of Fundamental & Applied Physics*, vol. 1, no. 2, pp. 24 -28, (2017).
- [34] Tangirala M., Zhang K., Nminibapiel D., Pallem V., Dussarrat C., Cao W., Adam T. N., Johnson C. S., Elsayed-Ali H. E. and Baumgart H., "Physical Analysis of VO₂ Films Grown by Atomic Layer Deposition and RF Magnetron Sputtering," *ECS Journal of Solid State Science and Technology*, vol. 3, no. 6, pp. N89-N94, (2014).
- [35] Wang X., Guo Z., Gao Y. and Wang J., "Atomic layer deposition of vanadium oxide thin films from tetrakis(dimethylamino)vanadium precursor," *JMR EARLY CAREER SCHOLARS IN MATERIALS SCIENCE ANNUAL ISSUE*, vol. 32, no. 1, (2017).
- [36] Currie M., Mastro M. A. and Wheeler V. D., "Atomic Layer Deposition of Vanadium Dioxide and a Temperature-dependent Optical Model," *Journal of Visualized Experiments*, vol. 135, no. e57103, (2018).
- [37] Peter A. P., Toeller M., Adelman C. and Schaeckers M., "Process study and characterization of VO₂ thin films synthesized by ALD using TEMAV and O₃ precursors," *ECS Journal of Solid State Science and Technology*, vol. 1, no. 4, pp. 169-174, (2012).
- [38] Mirbagheri G., "Hyperbolic Metamaterial Filter for Angle-Independent TM Transmission in the Infrared Regime," *NanoMeter The Newsletter of the Cornell Nano Scale Facility*, vol. 29, no. 2, p. 17, (2020).